Pure Appl. Chem., Vol. 80, No. 11, pp. 2377–2395, 2008.
doi:10.1351/pac200880112377

Polyaniline–carbon nanotube composites*

Pandi Gajendran and Ramiah Saraswathi‡

Department of Materials Science, Madurai Kamaraj University, Madurai 625 021, Tamil Nadu, India

Abstract: The key developments in polyaniline–carbon nanotube (PANI–CNT) composites are reviewed. Apart from in situ chemical polymerization and electrochemical deposition, a number of interesting approaches including the use of aniline functionalized CNTs and ultrasound/microwave/γ-radiation initiated polymerization have been used in the preparation of composites. The structure and properties of these composites have been investigated by a variety of techniques including absorption, infrared (IR), Raman, X-ray photoelectron spectroscopy methods, scanning electron and scanning probe microscopy techniques, cyclic voltammetry, and thermogravimetry. The experimental results indicate favorable interaction between PANI and CNTs. The CNT content in these composites controls their conductive, mechanical, and thermal properties. The most interesting characteristic is their easy dispersibility in aqueous solution. The performance evaluation studies of PANI–CNT composites in a number of applications including supercapacitors, fuel cells, sensors, and actuators are highlighted.

Keywords: polyaniline; conducting polymers; carbon nanotubes; composites; electroactive polymers.

INTRODUCTION

Electroactive polymers have been an area of immense interest over the past 30 years since the first discovery of conducting polyacetylene in 1977 by Shirakawa et al. [1]. Extensive research on several conjugated polymers including poly(*p*-phenylene), polyaniline (PANI), polypyrrole, polythiophene, polyindole, polycarbazole, polyfluorene, poly(*p*-phenylenevinylene), and their substituted derivatives have led to their applications in rechargeable batteries, microelectronics, sensors, electrochromic displays, and light-emitting and photovoltaic devices [2,3]. Among the various conjugated polymers, PANI (Scheme 1) has received special recognition owing to its good stability and interesting redox behavior [4–9]. In the past few years, several novel methodologies have been developed for the preparation of nanostructured PANI in the form of dispersions, nanowires, nanofibers, and nanotubules [10–16].

*Paper based on a presentation at the 3rd International Symposium on Novel Materials and Their Synthesis (NMS-III) and the 17th International Symposium on Fine Chemistry and Functional Polymers (FCFP-XVII), 17–21 October 2007, Shanghai, China. Other presentations are published in this issue, pp. 2231–2563.

‡Corresponding author

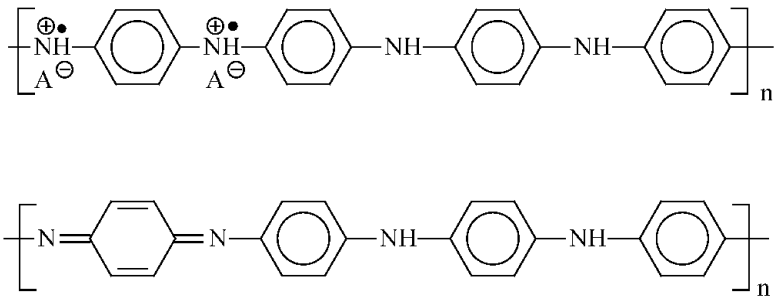

Scheme 1 ES and EB forms of PANI.

The discovery of fullerenes [17] and carbon nanotubes (CNTs) [18] has led to an explosion of research in nanoscience and nanotechnology. In fact, the focus in nanoscience has since shifted from synthesis to applications. A logical extension is to find new combinations of the existing materials as hybrid materials, blends, and nanocomposites for exploitation of their complementary properties [19–22]. In this context, there has been a new surge of interest in developing conducting polymer–CNT composites as novel futuristic materials. One main reason for this is that common applications of the two components offer the possibility to observe synergetic effects. Already, various studies have proved that certain discrete properties of the components of conjugated polymer–CNT composites are enhanced, thus validating their high suitability for some technological applications [23,24].

This review focuses mainly on the extensive literature published since 1999, on the preparation, characterization, and applications of PANI–CNT nanocomposites. The possible interactions between PANI and CNT that may be responsible for enhancement in certain properties of the composites are highlighted. Wherever applicable, the literature on CNT composite materials with substituted derivatives of PANI is also included.

PREPARATIVE METHODS

Since the first report in 1999 on the efficient electropolymerization of aniline on CNT whiskers [25], a number of innovative methodologies have been developed for preparing PANI–CNT composites. A general scheme of the common preparative methods is given (Scheme 2).

Apart from direct solid-state mixing [26] and dispersal of CNTs in PANI solutions of *N*-methyl-2-pyrrolidinone [27] or HCl [28], several chemical and electrochemical procedures have been reported. A simple method is in situ chemical polymerization of aniline in an acidic dispersion of multiwall carbon nanotubes (MWCNTs) or single-wall carbon nanotubes (SWCNTs) in the presence of an oxidant at low temperature [29,30]. The in situ chemical polymerization has been used also in the preparation of composites of substituted PANI like poly(*o*-anisidine) [31], poly(*N*-methylaniline) [32], poly(diphenylamine) [33], and poly(*o*-aminobenzoic acid) [34] with either SWCNTs or MWCNTs.

1. **Direct mixing**

a) **Solid–State Mixing**

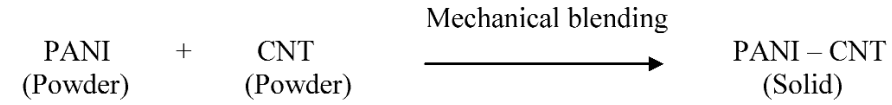

b) **Solution Mixing**

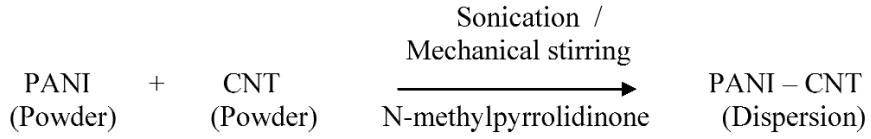

2. ***In situ* Chemical Polymerization**

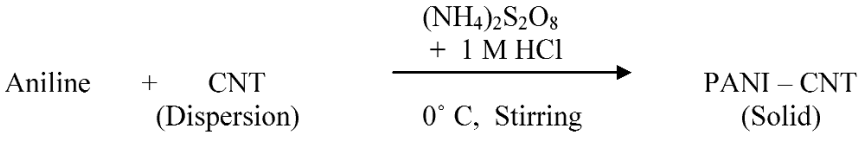

3. **Electrochemical Polymerization**

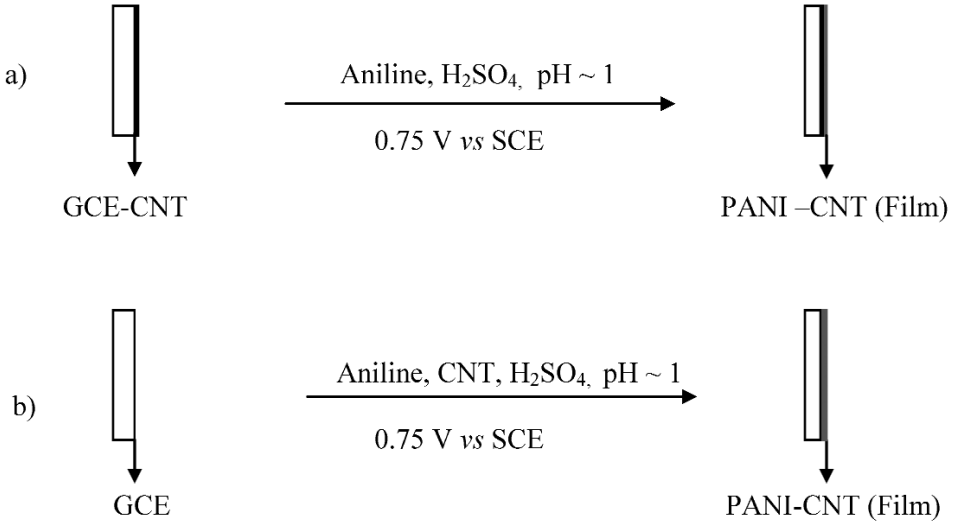

Scheme 2 Generalized scheme of preparative methods of PANI–CNT composites.

Chemical functionalization of MWCNTs with an acyl chloride group has been used to increase the interfacial binding between CNTs and PANI [35]. In a similar way, a nanotubular composite has been prepared using *p*-phenylenediamine functionalized MWCNT [36,37]. A sulfonated MWCNT can be used as the self-assembled template in the formation of PANI nanostructures [38]. A water-soluble self-doped PANI–SWCNT composite has been obtained by in situ polymerization of 3-aminophenylboronic acid monomer in the presence of DNA-functionalized SWCNT [39]. Nanocables of PANI–CNT composites can be obtained by the chemical oxidative polymerization of aniline from aqueous dispersions of CNT containing a sufficiently high concentration of a cationic surfactant like cetyltrimethylammonium bromide or a non-ionic surfactant like poly(ethylene glycol)mono-*p*-nonyl phenyl ether [40,41]. In situ chemical polymerization in an aqueous emulsion mixture containing a small quantity of dimethylbenzene has been carried out in the presence of CNT and sodium dodecylbenzene sulfonate [42]. The use of poly(vinyl alcohol) as stabilizer in the composite preparation has been reported [43]. An in situ inverse microemulsion route using sodium dodecylbenzene sulfonate has resulted in the formation of a core-shell PANI–MWCNT nanocomposite (Scheme 3) [44]. An optically active PANI–CNT composite has been prepared by in situ polymerization in the presence of (*S*)-(+)-10-camphorsulfonic acid [45–47]. A post-sulfonation procedure with chlorosulfonic acid in 1,2-dichloroethane has been adopted to prepare a water-soluble composite [48]. The effects of ultrasound, microwave, and γ-radiations on the formation of PANI–CNT composites have been explored [49–52].

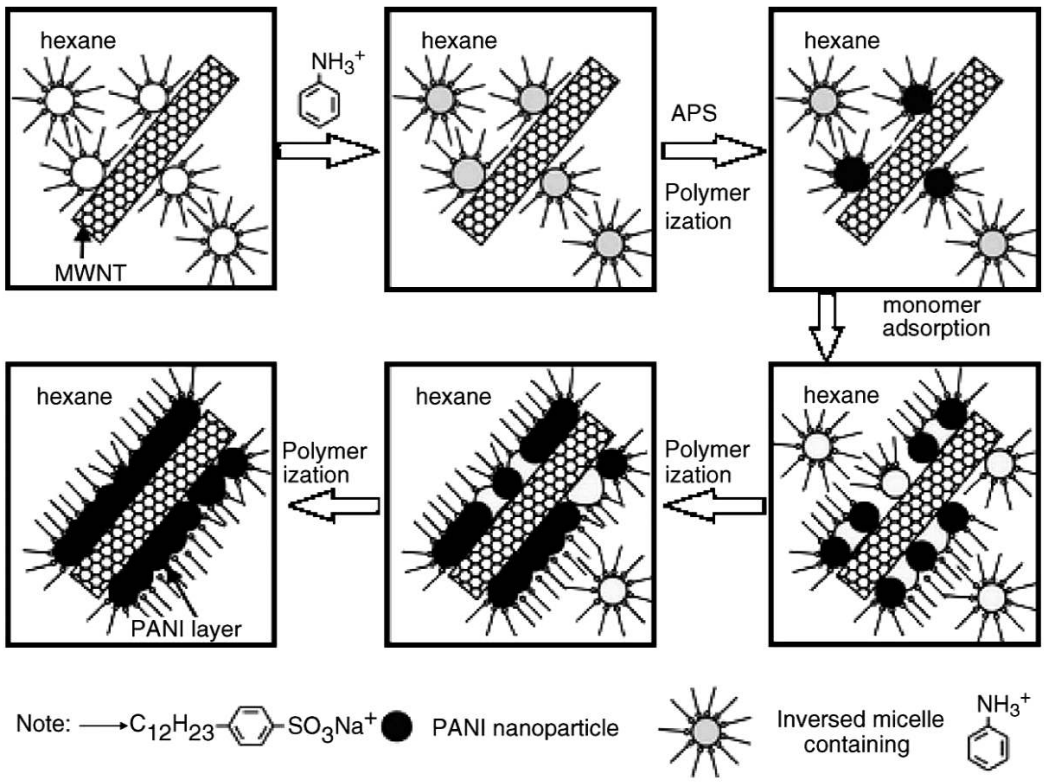

Scheme 3 Preparation of PANI–CNT core-shell nanocomposite by inverse microemulsion route (reproduced from ref. [44]).

Electrochemical deposition is another viable approach for the preparation of PANI–CNT composites. The initial attempt has been the direct electrochemical polymerization of aniline on individual CNT whiskers [25]. Another approach has been the electropolymerization of aniline from an aqueous dispersion containing aniline and CNT [53]. Sometimes, the aniline functionalized CNT has been dispersed in the electrolyte [54]. Substituted PANI can be grafted to SWCNT by oxidative coupling during electropolymerization [55,56]. A layer-by-layer method has been employed to form a multilayer film of CNT and PANI by alternatively drop-casting MWCNT dispersion followed by electrodeposition of aniline [57]. However, in such bilayer matrices, there is a possibility that the top PANI layer might block the functional capability of CNT. To overcome this difficulty, a MWCNT-grafted PANI has been proposed [58]. Recently, a novel procedure for the electrodeposition of a chiral PANI–CNT composite film on different substrates like gold on silicon chip, indium tin oxide-coated glass plate, and carbon rod has been reported. The optical activity of the composite can be tuned by the selection of either electrode materials or CNT content in the electrolyte [59]. A donor–acceptor PANI–SWCNT or MWCNT dyad has been obtained electrochemically in an ionic liquid, 1-butyl-3-methyl-imidazolium hexafluorophosphate, containing 1 M CF_3COOH [60,61].

In some studies, the CNT has been mixed with a binder like poly(vinylidene difluoride) (PVDF) to increase its adherence to the electrode substrate [62,63]. Alternatively, a light suspension of CNT in a surfactant solution can be sprayed onto the substrate for further electropolymerization [64,65]. However, the use of such binder/surfactant in electrode preparation may increase the substrate resistance. A simple and direct procedure for the electrochemical preparation of PANI–CNT composites is the direct drop-casting of an aqueous dispersion of acid-treated MWCNT on a glassy carbon electrode for subsequent polymerization of aniline [66].

A nanohybrid based on CNT–PANI–nickel hexacyanoferrate and an organized multilayer assembly consisting of a network of PANI-linked polyoxometallate-stabilized CNTs have been prepared [67,68]. Such multifunctional composites will be useful in sensor applications.

CHARACTERIZATION STUDIES

The PANI–CNT composites have been characterized by electrochemical, microscopic, spectral, conductivity, and thermal measurements. However, very few studies have monitored the changes in their redox, electrical, thermal, and mechanical properties with different loading of CNT. In general, the properties of these composites greatly depend on their method of preparation and CNT content.

Despite the insoluble nature of PANI in water, PANI–CNT composites can be readily dispersed in aqueous solutions (Fig. 1). The CNT used in many of the preparative schemes of these composites has been subjected to a 1:3 nitric acid–sulfuric acid mixture treatment. This process results in the conversion of a hydrophobic CNT to a hydrophilic one due to the incorporation of acid functionalities [69]. As a consequence, the PANI–CNT composites containing the hydrophilic CNT become water-dispersible.

The cyclic voltammetric peak potentials of PANI–CNT composites show very small and insignificant shifts compared to those of pure PANI although there is a considerable increase in peak currents [53,66,70,71]. The absence of any change in the peak potentials suggests that the mechanism of aniline polymerization is not affected in the presence of CNT [71]. Impedance studies have shown considerable decrease in the charge-transfer resistance with increasing content of CNT [72].

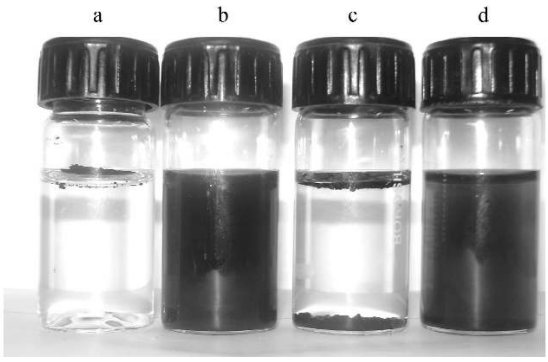

Fig. 1 Photographs showing the solubility of MWCNT and PANI–CNT composite in water: (a) MWCNT before functionalization; (b) MWCNT after functionalization; (c) PANI; and (d) PANI–MWCNT composite.

Scanning electron microscopy (SEM) is an excellent technique for investigating the morphology of PANI–CNT composites. In general, the SEM characterization of these composites reveals a uniform wrapping of CNT by PANI forming core-shell nanostructures (Fig. 2) [44,61,66,73]. The shell diameter depends on PANI content in the composites. Gupta and Miura have reported that beyond 73 wt % of PANI, the wrapping gets terminated and the PANI is deposited independently around the surface of the composite [62]. Scanning tunneling microscopy (STM) [74], atomic force microscopy (AFM) [75–77], and transmission electron microscopy (TEM) techniques [45,46] have been used in morphological characterization, and the results of these studies also reveal a nice encapsulation of CNT by the polymer.

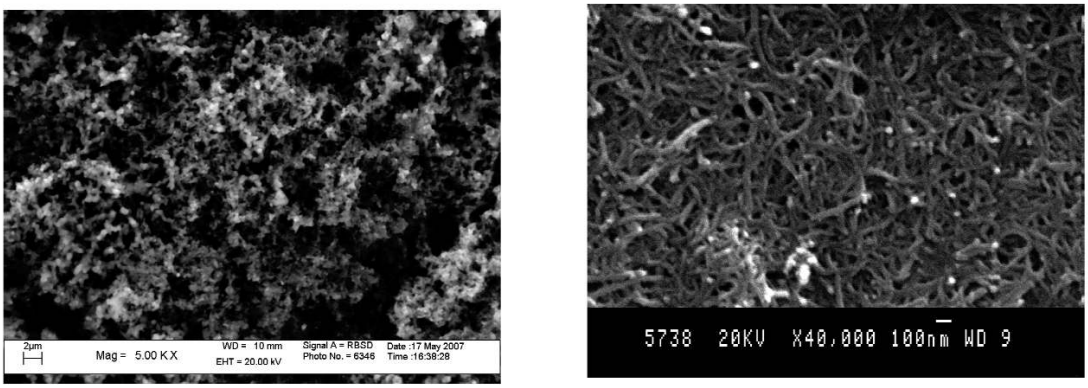

Fig. 2 SEM images of electrochemically deposited (a) PANI and (b) PANI-CNT composite.

The UV–vis spectral characterization of the composites of MWCNT with emeraldine salt (ES) and emeraldine base (EB) forms of PANI in *N*-methyl-2-pyrrolidinone has been reported [45]. The EB form gives two peaks with maxima at 320 and 620 nm corresponding to π–π* transition centered on the benzenoid unit and quinonoid exciton band, respectively, whereas the ES form shows characteristic absorption bands at 345, 415, and 810 nm associated with π–π*, polaron-π*, and π–polaron transitions, respectively. The introduction of MWCNT in PANI (ES or EB) results in the appearance of a new band around 290 nm [45,75]. In addition to this, there is a considerable blue shift of about 30 nm of the π–π* transition band. The polaron bands remain unaffected.

Detailed structural investigations of PANI–CNT composites by FT–IR spectroscopy have been reported. The composites prepared by in situ polymerization contain all the characteristic peaks of PANI in its ES form. For example, the spectrum shows N–H stretching vibration (3450 cm^{-1}), C=C stretching of quinonoid (Q, 1576 cm^{-1}) and benzenoid (1493 cm^{-1}), C–N stretching mode (1303 cm^{-1}), and N=Q=N stretching (1136 cm^{-1}) [46]. In addition to the above, the presence of CNT in these composites results in the appearance of a band at 1144 cm^{-1} whose intensity increases with CNT content [27]. Another important observation is the reversal of the relative intensity of the quinonoid and benzenoid bands in the composites compared to pure PANI. The intensity of the quinonoid band is higher than that of benzenoid band, revealing that PANI in these composites is richer in quinonoid units. The π-bonded surface of CNT interacts strongly with the conjugated structure of PANI, especially through quinonoid rings [78].

The Raman spectral data agree with the results obtained by infrared (IR) spectroscopy. The Raman spectral characterization of the composites can be very valuable in understanding the specific interactions between PANI and CNT. The Raman lines of the ES form of PANI appear at 1175, 1260, 1330–1380, 1484, 1589, and 1618 cm^{-1} corresponding to C–H bending in benzenoid ring, C–H bending in quinonoid ring, semiquinone radical, C=N, C=C, and C–C stretchings, respectively [79]. The Raman spectrum of the acid-treated CNT shows a strong phonon-induced high-frequency band at 1580 cm^{-1} (G mode) and another band originating from the defects in CNT at 1355 cm^{-1} (D mode). In the low-frequency region, a characteristic Raman line at 178 cm^{-1} (radial breathing mode, RBM) is observed. The chemical modification of the MWCNT does not change the band positions but can vary the relative intensity of the bands [35]. The Raman spectra of PANI–CNT composites contain all the characteristic peaks of PANI with their band positions virtually unchanged. The intensities of the peaks at 1175, 1330, and 1484 cm^{-1} increase with increasing content of CNT, indicating strong interaction between quinonoid rings and CNT. However, the D and G lines corresponding to CNT are not observed. Wei et al. have reported that the Raman lines of CNT totally disappear in the composites due to the complete coverage of CNT surface by PANI [61].

X-ray photoelectron spectral investigation of the composites reveal an enhancement in their intrinsic oxidation state. These composites have a higher polymeric degree with a lower defect density [30,49,71]. X-ray powder diffraction analysis shows no new peaks in PANI–CNT composites. The ES form of PANI shows crystalline peaks centered at $2\theta = 9.4°$, 15.3°, 20.7°, 25.2°, 26.5°, and 29.8° corresponding to (001), (011), (020), (200), (121), and (022) reflections, respectively [35]. The as-prepared sample of MWCNT by chemical vapor deposition shows three peaks at $2\theta = 26°$, 39.6°, and 43° [46]. However, the acid-treated and –COOH-functionalized sample of MWCNT shows only two diffraction peaks at $2\theta = 26°$ and 46° [35]. The X-ray data of PANI–CNT composites show all the peaks corresponding to PANI as well as CNT, which reveal that no additional crystalline order is introduced in these composites [29,35].

SALIENT PROPERTIES

The density value of PANI–CNT composite increases from 1.33 to 1.9 g cm^{-3} when the CNT loading is gradually changed from 0 to 100 wt %. However, the density of a mixture of PANI and CNT obtained by mechanical blending shows a decreasing trend with increasing CNT loading suggesting the formation of macropores within the sample [73].

The room-temperature conductivity of well-aligned PANI–CNT composites increases by one order of magnitude compared to that of PANI. The conductivity value decreases with decreasing temperature, exhibiting typical semiconductor behavior. The temperature dependence of the resistivity is weaker than the one for PANI, suggesting that the delocalization of charge carriers is greater in the nanocomposites [80]. The average localization length of the composites increases with increasing CNT content. The negative magnetoresistance provides strong evidence to support the observation that the average localization length is enhanced and the electronic transport is dominated by CNT [81]. The con-

ductivity of poly(*m*-aminobenzene sulfonic acid)–SWCNT graft copolymers has been shown to be about four orders of magnitude higher than that of the neat polymer [34]. The acid-functionalized CNT can change dramatically the electrical properties of PANI–CNT composites [82]. Haddon's group has reported the important role that chemical functionalization of CNT can play in modifying the electronic properties of PANI–CNT composites [83].

The current–voltage (*I–V*) measurements performed on Schottky diodes have shown rectification for both PANI and PANI–SWCNT composites, but the current for the composite diode is significantly larger than that of pure PANI device [84]. The *I–V* curve shows two distinct regions. At lower voltages, the mechanism follows Ohm's law, and at higher voltages, the mechanism is consistent with space-charge limited emission [85,86].

The thermal stability of PANI–CNT composites is somewhat better than that of doped PANI. The synthesis method and the degree of graphitization of CNT affect the decomposition behavior of these composites [44,49]. Doped PANI exhibits a three-step decomposition viz. release of water molecules (<100 °C), dopant anion (180–280 °C), and decomposition of PANI (280–630 °C) [87]. The decomposition of MWCNT occurs anywhere between 500 and 850 °C depending on the method by which it is synthesized [46]. A 1 wt % MWCNT content in PANI–CNT composites extends the onset of decomposition from 280 to 400 °C. The decomposition temperature can be increased with increasing content of CNT in the composites (Fig. 3). In some studies, the formation of a new phase in these composites is identified by the presence of another additional weight loss step at about 590 °C [44].

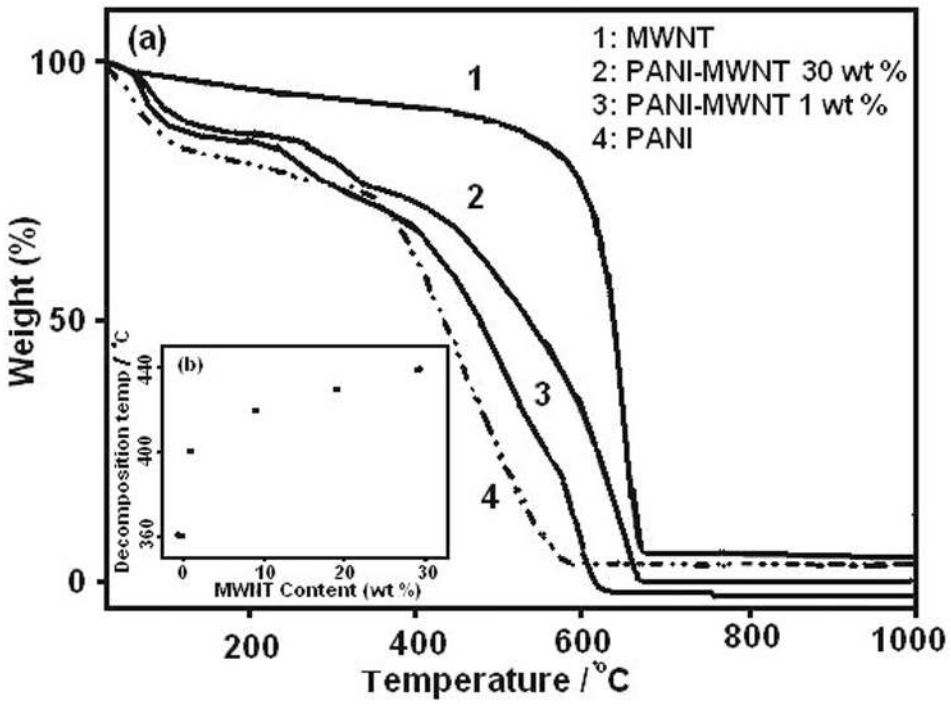

Fig. 3 (a) TGA curves of the MWCNT, PANI–MWCNT 30 wt %, PANI/MWCNT 1 wt %, and PANI. (b) Plot of decomposition temperature of composites with different MWCNT content (reproduced from ref. [44]).

One of the main motivation factors in preparing PANI–CNT composites has been that the mechanical properties of the polymer can be greatly enhanced due to its integration with CNT. The tensile strength of dedoped and doped PANI fibers is in the range of 95–157 MPa. For a 2 wt % CNT loading, the tensile strengths are 260 MPa before polymer doping and 197 MPa after doping. For the same CNT

loading, the Young's modulus of PANI–CNT fibers are up to 17 GPa, which is much higher than the value of 2–4 GPa for PANI. Also, there is a 30 % decrease in elongation at break [88,89]. However, in the case of PANI–CNT films, the modulus decreases as the CNT content is increased, while the per cent strain increases from 12 % for neat PANI to 30 % for the composite with 1 % CNT. But the per cent strain decreases to 11 % for a 5 % CNT loading indicating that the composite films become more brittle when loaded in excess of 1 % CNT [90]. The dispersion of PANI–MWCNT composite with 1 wt % polyvinyl alcohol in insulating silicone oil behaves like an electrorheological fluid. The shear stress of the dispersion increases with an increase in applied DC electric field for a broad range of shear rates [91–93]. A composite of *p*-tolunesulfonic acid-doped PANI–MWCNT shows good microwave absorption [94].

INTERACTIONS BETWEEN PANI AND CNT

The electrical, thermal, and mechanical properties of PANI–CNT composites are intermediate between pure PANI and CNT but vary depending on CNT content and the extent of its integration with PANI. However, it is exceptional that the electrochemical properties of these composites are tremendously enhanced compared to the two individual components. For example, despite the same surface area, the electrochemical growth, redox and capacitive currents of the composites are several-fold higher compared to the values obtained on pure PANI (Fig. 4) [66,70]. Such a remarkable enhancement in electrochemical properties appears to be unique to PANI–CNT composites and has not been observed for any other conjugated polymer–CNT composites. Composites of CNT with substituted PANI derivatives also show electrochemical current enhancements, but the extent of the increase depends on the nature of the substituent present in the aniline ring [95].

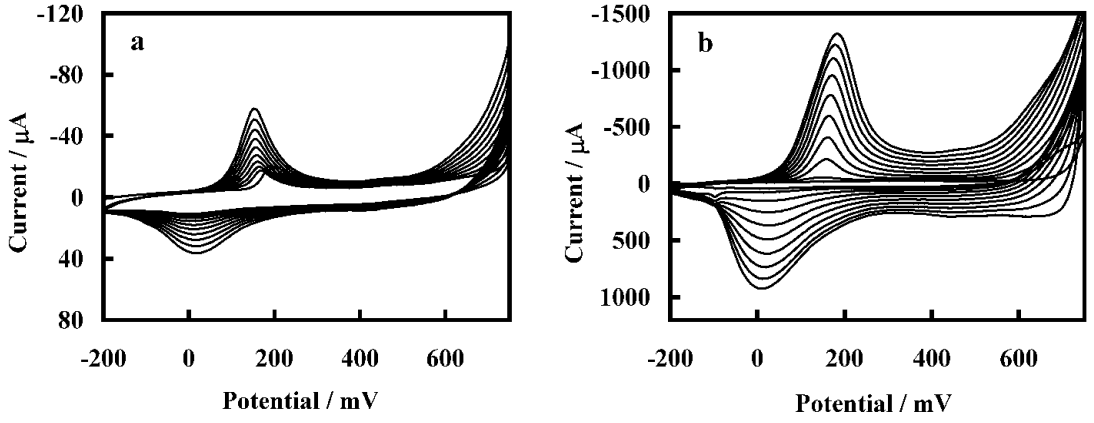

Fig. 4 Current enhancement during cyclic voltammetric growth of PANI at (a) GCE (0.07 cm^2) and (b) CNT/GCE (0.07 cm^2); electrolyte: 0.5 M aniline in 1 M H_2SO_4; sweep rate: 50 mV s^1.

Several studies have dealt with the various possible interactions between PANI and CNT in the composites. One of the first suggestions has been the attachment of aniline radicals, generated during electrochemical oxidative polymerization, onto the CNT lattice especially at defect sites resulting in local deposits which grow in size and finally become interconnected to form a multilayer coating [55]. The carboxylic sites at the acid-treated CNT are the most likely sites of interaction with aniline monomer [66]. Huang et al. have proposed the formation of a charge-transfer complex between the electron-accepting CNT and the electron-donating aniline on the basis of formation of new peaks at 362, 455, 510, and 550 nm in the UV–vis absorption spectra [54]. A Fourier transform–infrared

(FT–IR) band at 1144 cm^{-1}, the intensity of which increases with increasing content of CNT, has been attributed to the charge transfer between PANI and CNT [27]. The possibility of charge transfer from the planar polymer chain to CNT via the highly reactive imine group has been also suggested [78]. Strong π–π interactions between the more planar PANI conformation and the hexagonal surface lattice of CNT are inevitable [75]. The π–π interactions may be the reason for the observed CNT core-polymer shell morphology or the CNT being wrapped by the polymer as revealed in the SEM characterization. Hydrogen bonding between the amino groups of aniline monomers and the carboxylic acid/acyl chloride groups of CNT has been also reported [35]. Simple adsorption of aniline monomers onto the surface of CNT has been suggested [36]. The carboxylic acid groups introduced on the sidewalls of the CNT by acid oxidative treatment have been shown to induce doping in PANI [78]. More detailed experimental results based on in situ spectroelectrochemical or scanning probe techniques may be necessary to have a consensus on the specific interaction between PANI and CNT in these composites. It is to be noted that the exceptional electrochemical properties of these composites will bear more value in the use of these materials in batteries and sensors and is the main factor responsible for the observed synergetic effects in these applications.

APPLICATIONS

A number of reports have appeared highlighting the synergetic performance of PANI–CNT composites in certain applications including fuel cells, supercapacitors, and sensors. The salient findings regarding these applications of the composites are given below.

Batteries and supercapacitors

There are only very few reports on the use of PANI–CNT composites in battery applications. Wang et al. have obtained a discharge capacity of 11.2 mAh/g for the composite of PANI nanofibers containing 0.25 wt % of CNT as cathode material in ethylmethyl imidazolium bis(trifluoromethanesulfonyl) amide ionic liquid as electrolyte [96]. The discharge capacity value of the composite is nearly threee times higher than that of pure PANI. In another study by Sivakkumar and Kim, a discharge capacity of 139 mAh/g has been reported for a cell assembled with pure PANI–CNT composite as cathode and lithium as anode in an electrolyte consisting of 1-ethyl-3-methylimidazolium tetrafluoroborate and vinylene carbonate [97]. The same group has used a gel polymer electrolyte based on porous poly(vinylidenefluororide-co-hexafluoropropylene), and the cell has yielded a discharge capacity of 86 mAh/g [98].

The application of PANI as a conducting polymer electrode in redox capacitors and CNT in double-layer capacitors are well known, and several reviews have been published [99–104]. The reported maximum capacitance is about 1300 F/g for PANI redox supercapacitor [105] and 180 F/g for CNT supercapacitor [102]. The commercially available supercapacitors are based on activated carbon with a capacitance value as high as 5000 F/g [103]. The incorporation of CNT into PANI matrix is expected to enhance its electrical and mechanical properties, which are essential for actual device fabrication. The use of PANI–CNT composite as an electrode in a hybrid capacitor has been suggested first by Frackowiak and Beguin [106]. In the past few years, many attempts have been made to improve the capacitance of PANI–CNT-based devices [107–114]. The details of the cell construction with the experimental values of capacitance obtained in these studies are presented in Table 1. The highest value obtained so far is 650 F/g with a stability of 1000 cycles [110].

Table 1 Capacitance data of PANI–CNT composites.

Electrode material	Electrolyte	Capacitance F/g	Cycle life	Ref.
Pressed pellet of SWCNT and poly(vinylidene chloride) (7:3) after pyrolysis at 1000 °C	7. 5 M KOH	180	–	[102]
Electrochemically deposited PANI on a stainless steel substrate	1 M $HClO_4$ + 3 M $NaClO_4$	1300	1000	[105]
Pressed pellet of PANI–MWCNT (80 wt %), acetylene black (15 wt %) and polytetrafluoroethylene (5 wt %)	1 M $NaNO_3$	328	1000	[107]
Electrochemically deposited PANI–SWCNT composite (8 wt % SWCNT) on a stainless steel substrate	1 M $HClO_4$ + 1 M $NaClO_4$	311	–	[108]
Pressed pellet of composite containing PANI (80 wt %) and MWCNT (20 wt %)	1 M H_2SO_4	650	1000	[110]
Pressed pellet of PANI–CNT (95 wt %) and polytetrafluoroethylene (5 wt %)	1 M $NaNO_3$	183	–	[111]
Electrochemically deposited PANI (73 wt %) on CNT–PVDF (9:1) film on stainless steel	1 M H_2SO_4	463	1500	[62,63]
Pressed pellet of 90 wt % PANI–MWCNT (74 wt % PANI nanofiber and 26 wt % MWCNT), carboxy-methyl cellulose (6 wt %) and styrene-butadiene rubber (4 wt %)	1 M H_2SO_4	606	200	[112]
Pressed pellet of 80 wt % PANI–MWCNT, carbon black (15 wt %), and polytetrafluoroethylene (5 wt %)	1 M H_2SO_4	322	–	[50]

Fuel cells

PANI–CNT composites can be used as efficient electrocatalytic materials in fuel cell reactions like oxygen reduction and methanol oxidation. The CNT provides higher surface area and better electronic conductivity while PANI facilitates the electron transfer through the conducting matrix. A PANI-grafted MWCNT composite has shown a 610 mV more positive current onset potential for the two-electron oxygen reduction with a 20-fold enhancement in amperometric current [115]. A poly(*o*-phenylenediamine)–MWCNT composite has shown a polymer redox-mediated electrocatalytic effect for oxygen reduction with a five-fold enhancement in current and a favorable potential shift of 130 mV compared to the values obtained at a pure poly(*o*-phenylenediamine) electrode [66].

The PANI–CNT composites can serve as excellent host matrices for metal nanoparticles. The metal-impregnated composites can be used as electrode materials in methanol oxidation reaction [115–118]. It has been established that the size of the metal nanoparticles deposited on the composite matrix is smaller than that on PANI. This gives a higher dispersion and better utilization of the metal nanoparticle-impregnated composites, resulting in their high performance and stability [71]. Apart from enhanced electrocatalytic activity, the PANI–CNT composites consisting of metal nanoparticles have shown a reduced poisoning effect from adsorbed carbon monoxide [116]. A platinum-incorporated poly(*o*-phenylenediamine)–MWCNT electrode has shown a two-fold catalytic activity toward methanol oxidation compared to a platinum-poly(*o*-phenylenediamine) electrode [118]. Platinum incorporated PANI–CNT composites have been shown to exhibit better electrocatalytic activity toward the oxidations

of formaldehyde and formic acid as well [119–121]. A microbial fuel cell with PANI–CNT composite as anode in 0.1 M phosphate buffer consisting of 5.5 mM of glucose, 2-hydroxy-1,4-naphthoquninone as mediator, and *Escherichia coli* bacteria as the microbial catalyst has been reported to give a cell voltage of 450 mV with a power density of 42 mW m^{-2} [122].

Sensors

The applications of both conducting polymer and CNT in chemical, gas, and biosensors have been widely demonstrated in literature, and there are excellent reviews on this topic [2,123–136]. The expected synergetic effect of PANI–CNT composites has been a motivating factor to do research on sensors, exploiting the mechanical stability of CNT and the redox properties of PANI.

A solid-state pH sensor using PANI–CNT composite has been reported [137,138]. The device is sensitive in the pH range between 1 and 13 and shows good sensitivity, linearity, and stability. A gas sensor based on poly(*o*-anisidine)–CNT composite offers a sensitivity of about 28 % compared to a mere 4 % by CNT alone for the detection of inorganic vapor, HCl [139,140]. The detection of triethylamine vapor has been also reported [141]. Sensors for the detection of carbon monoxide in the concentration range of 0.01–1000 ppm have been developed [142,143].

The response of PANI–CNT composites in the detection of nitrite has been studied. A linear range from 5 μM to 15 mM has been observed with a detection limit of 1 μM [144]. A poly(*o*-phenylenediamine)–MWCNT composite exhibits a 16–fold enhancement with a 450 mV favorable potential in nitrite detection [95]. A CNT–PANI–nickel hexacyanoferrate composite shows a high selectivity for cesium ions over sodium ions. This may find application in the removal of cesium from radioactive wastes [145]. A poly(1,2-diaminobenzene)–CNT nanoporous composite can be used in the simultaneous voltammetric determination of trace level of cadmium and copper ions with detection limits between 0.25 and 0.33 ppb, respectively [146]. Recently, PANI–MWCNT composite has been used in the detection of acetaminophen in acetate buffer up to a limit of 2.5×10^{-7} M [147]. A biosensor based on the composite of pyrene sulfonic acid-functionalized SWCNT embedded in PANI has shown two- to six-fold enhancement depending on applied potential, compared to polystyrene sulfonate-doped PANI in the detection of glucose [148]. A multilayer composite film consisting of the EB form of PANI and poly(aminobenzenesulfonic acid)-functionalized SWCNT can detect β-nicotinamide adenine dinucleotide (NADH) at a much lower potential. For a six-bilayer electrode, the detection limit can be as low as 10^{-5} M [149]. Another sensor for NADH has been developed with poly(1,2-diaminobenzene)–MWCNT composite in a range from 2 μM to 4 mM [150]. A CNT composite of poly(anilineboronic acid) functionalized with single-strand DNA (ss-DNA) shows great promise for the effective detection of dopamine of concentration as low as 40 pM without any interference from ascorbic acid [77,151,152]. Similarly, a PANI-β-cyclodextrin-MWCNT composite can be used for the selective detection of dopamine up to 1.2×10^{-8} M in the presence of ascorbic acid [153]. The PANI–MWCNT–gold nanocomposite film exhibits good electrocatalytic activity toward ascorbic acid [154]. Enhanced sensitivity toward a glucose biosensor by a gold electrode-modified poly(*o*-aminophenol)–MWCNT composite has been reported [155]. PANI-grafted MWCNT and also polydiphenylamine-grafted MWCNT composite electrodes display good electrocatalytic response in the detection of H_2O_2 [58,156]. A sensor based on PANI–prussian blue–MWCNT composite for the detection of H_2O_2 has been also developed. The sensitivity is three orders of magnitude higher than the reported value so far [157]. A glucose biosensor constructed by immobilizing glucose oxidase with nafion and glutaraldehyde onto the PANI–prussian blue–MWCNT composite gives a detection limit of 0.01 mM for glucose [158]. The PANI–MWCNT composite offers a significant decrease in the overvoltage for the H_2O_2 reduction. A biosensor for the detection of choline without any interference due to ascorbic acid and uric acid has been developed [57].

Actuators

The PANI–CNT composites have received a good deal of attention as smart materials in high-strength actuators which directly convert electrical energy into mechanical energy. Dubbed as artificial muscles, these electrochemomechanical devices can find applications in robotics, optical fiber switches, optical displays, prosthetic devices, microscopic pumps, and antivibration systems. Conducting polymers like PANI and polypyrrole have been extensively investigated for applications in artificial muscles [159–162]. However, one deficiency of conducting polymer actuators has been their low actuating strain and small force outputs. The PANI–CNT composites can have an improved performance in actuators because of their high Young's modulus and electrical conductivity.

Since the first report by Baughman et al. [163] on the use of SWCNT as actuator material, several detailed research reports have appeared [164–166]. It should be mentioned here that the actuations of PANI and CNT occur due to different mechanisms. Non-faradaic charging of CNT is the main factor for actuation of CNT while the polymer redox reactions are responsible for actuation effects in PANI.

The actuator behavior of PANI–CNT composites has been investigated in detail by the Wallace group [167–170]. A PANI–CNT composite (1:3 by wt) has an enhanced actuation strain ranging from 0.2 to 0.5 % compared to 0.06 % of pure CNT [167]. The electrolyte has a role on the actuation behavior. An aqueous solution of 1 M $NaNO_3$ can give good actuation stability independent of the applied stress [168]. SWCNT (2 wt %) reinforced PANI fibers can sustain stress up to 1 MPa, which is three times higher than pure PANI fibers [169]. A dual-mode actuation has been reported for a composite containing fibers of chitosan, PANI, and SWCNT. The activation depends on pH changes and redox polymer reactions. Such dual-mode actuators are expected to have design advantages in the construction of microelectromechanical systems (MEMS) [170]. A hybrid actuator based on cellulose–PANI–CNT composite has been studied. The effects of the wt % of MWCNT in the composite and sonication time used in its preparation on the actuation bahavior have been investigated in detail [171–173].

Other applications

PANI can be used as a dopant to convert a *p*-type CNT field-effect transistor (CNTFET) to a *n*-type device [174]. Ramamurthy et al. have reported that PANI containing 1 % CNT is suitable for organic device applications [175]. A PANI–SWCNT composite has been proposed for high-resolution printable conductors for applications in organic electronics. PANI doped with dinonylnaphthalene sulfonic acid (DNNSA–PANI) can be robust to withstand the heat generated in the imaging process without degradation in conductivity. The DNNSA–PANI–SWCNT composite is suitable to print micron-size channels with high resolution at high speeds via laser ablation without the need for the wet chemistry or photolithography [176,177]. A water-dispersible PANI composite with a MWCNT loading of about 32 % is the ideal formulation for inkjet printing. The printed films possess good optical transparency, sheet resistance, and electrochromic behavior, allowing switching between yellow, green, and blue [178]. Exploiting the readily dispersible nature of the PANI–CNT composites in aqueous medium, it has been demonstrated that a conventional dyeing process can be effectively applied to incorporate CNT instead of metal into textiles with a water-soluble poly(2-methoxyaniline-5-sulfonic acid)–SWCNT composite as the dye [179]. Transparent SWCNT film on a polyethylene terephthalate substrate can be used to replace the acid-sensitive Sn-doped In_2O_3 for PANI-based electrochromic devices [180].

CONCLUSIONS AND FUTURE PROSPECTS

This review has dealt with the specific literature on PANI–CNT composites. To our knowledge, this is the first concise effort to present a summary of the preparative methods, characterization data, and ap-

plications of these novel nanocomposites. Among the various preparative methods, the electrochemical method appears to be more promising to obtain these composites with superior redox properties, which are essential for certain electrochemical applications like sensors and actuators. However, there are other methods like template synthesis and self-assembly, which remain to be explored. Methods should be devised also to prepare free-standing films. The synthesis of the composites in nonaqueous media also remains a challenge. More importantly, the extensive possibility of functionalizing the CNT should pave way for the preparation of new PANI–CNT composites. The acid-treated CNT is suitable for providing a better interaction with PANI. The integration of PANI with the acid-treated CNT in the form of a composite material has resulted in a simple procedure for dissolving the doped PANI in aqueous solutions. Almost all the properties of the composites depend on the method of their preparation and also on CNT content. Unlike other conducting polymers like polypyrrole or polythiophene, PANI has shown strong interactions with CNT, resulting in a synergetic performance of the composites in several applications. Among the tested applications, the composites appear to be more suitable for electrocatalysis and sensors. There is a lot of scope for the better use of these composites in biosensors, microelectronics, and membrane technology.

ACKNOWLEDGMENT

The financial assistance from DST, CSIR, INSA, and UGC under the university with potential for excellence scheme is gratefully acknowledged.

REFERENCES

1. H. Shirakawa, E. J. Louis, A. G. MacDiarmid, C. K. Chiang, A. J. Heeger. *J. Chem. Soc., Chem. Commun.* 578 (1977).
2. T. A. Skotheim, R. L. Elsenbaumer, J. R. Reynolds (Ed.). *Handbook of Conducting Polymers*, 2nd ed., Marcel Dekker, New York (1998).
3. P. Chandrasekhar. *Conducting Polymers, Fundamentals and Applications*: *A Practical Approach*, Kluwer Academic, Boston (1999).
4. E. M. Genies, A. Boyle, M. Lapkowski, C. Tsintavis. *Synth. Met.* **36**, 139 (1990).
5. A. A. Syed, M. K. Dinesan. *Talanta* **38**, 815 (1991).
6. D.C. Trivedi. In *Handbook of Organic Conducting Molecules and Polymers*, H. S. Nalwa (Ed.), 2, Chap. 12, John Wiley, New York (1997).
7. E. T. Kang, K. G. Neoh, K. L. Tan. *Prog. Polym. Sci.* **23**, 277 (1998).
8. N. Gospodinova, L. Terlemezyan. *Prog. Polym. Sci.* **23**, 1443 (1998).
9. A. Malinauskas. *J. Power Sources* **126**, 214 (2004).
10. R. Gangopadhyay. In *Encyclopaedia of Nanoscience and Nanotechnology*, H. S. Nalwa (Ed.), 2, pp. 105–131, American Scientific Publishers (2004).
11. S. Neves, W. A. Gazotti , M. A. D. Paoli. In *Encyclopaedia of Nanoscience and Nanotechnology*, H. S. Nalwa (Ed.), 2, pp. 133–152, American Scientific Publishers (2004).
12. M. Wan. In *Encyclopaedia of Nanoscience and Nanotechnology*, H. S. Nalwa, (Ed.), 2, pp. 153–169, American Scientific Publishers (2004).
13. G. G. Wallace, P. C. Innis, L. A. P. Kane-Maguire. In *Encyclopaedia of Nanoscience and Nanotechnology*, H. S. Nalwa (Ed.), 4, pp. 113–130, American Scientific Publishers (2004).
14. D. Zhang, Y. Wang. *Mater. Sci. Eng. B* **134**, 9 (2006).
15. J. Jang. *Adv. Polym. Sci.* **199**, 189 (2006).
16. J. Huang. *Pure Appl. Chem.* **78**, 15 (2006).
17. H. W. Kroto, J. R. Heath, S. C. O'Brien, R. F. Curl, R. E. Smalley. *Nature* **318**, 162 (1985).
18. S. Ijima. *Nature* **354**, 56 (1991).

19. G. Kickelbick. *Hybrid Materials: Synthesis, Characterization and Applications*, Wiley-VCH, Darmstadt (2007).
20. J. Anand, S. Palaniappan, D. N. Sathyanarayana. *Prog. Polym. Sci.* **23**, 993 (1998).
21. A. Pud, N. Ogurtsov, A. Korzhenko, G. Shapoval. *Prog. Polym. Sci.* **28**, 1701 (2003).
22. R. Gangopadhyay, A. De. *Chem. Mater*. **12**, 608 (2000).
23. M. Baibarac, P. G. Romero. *J. Nanosci. Nanotechnol.* **6**, 289 (2006).
24. L. Dai. *Aust. J. Chem*. **60**, 472 (2007).
25. C. Downs, J. Nugent, P. M. Ajayan, D. J. Duquette, K. S. V. Santhanam. *Adv. Mater*. **11**, 1028 (1999).
26. I. A. Tchmutin, A. T. Ponomarenko, E. P. Krinichnaya, G. I. Kozub, O. N. Efinov. *Carbon* **41**, 1391 (2003).
27. M. Baibarac, I. Batlog, S. Lefrant, J. Y. Mavellec, O. Chauvet. *Chem. Mater.* **15**, 4149 (2003).
28. X. Bi, Z. J. Han, Y. Yang, B. K. Tay. *J. Phys. Chem. C* **111**, 4125 (2007).
29. M. Cochet, W. K. Maser, A. M. Benito, M. A. Callejas, M. T. Martinez, J. M. Benoit, J. Schreiber, O. Chauvet. *Chem. Commun.* 1450 (2001).
30. M. R. Karim, C. J. Lee, Y. Y. Park, M. S. Lee. *Synth. Met*. **151**, 131 (2005).
31. B. Valter, M. K. Ram, C. Nicolini. *Langmuir* **18**, 1535 (2002).
32. X. Lu, J. Zheng, D. Chao, J. Chen, W. Zhang, Y. Wei. *J. Appl. Polym. Sci*. **100**, 2356 (2006).
33. X. Lu, D. Chao, J. Zheng, J. Chen, W. Zhang, Y. Wei. *Polym. Int*. **55**, 945 (2006).
34. (a) B. Zhao, H. Hu, R. C. Haddon. *Adv. Funct. Mater.* **14**, 71 (2004); (b) B. Zhao, H. Hu. A. Yu, D. Perea, R. C. Haddon. *J. Am. Chem. Soc*. **127**, 8197 (2005).
35. T. M. Wu, Y. W. Lin. *Polymer* **47**, 3576 (2006).
36. B. Philip, J. Xie, J. Abraham, V. Varadan. *Polym. Bull*. **53**, 127 (2005).
37. B. Philip, J. Xie, J. K. Abraham, V. K. Varadan. *Smart Mater. Struct.* **15**, N105 (2004).
38. Z. Wei, M. Wan, T. Lin, L. Dai. *Adv. Mater.* **15**, 136 (2003).
39. Y. Ma, S. R. Ali, L. Wang, P. L. Chiu, R. Mendelsohn, H. He. *J. Am. Chem. Soc*. **128**, 12064 (2006).
40. X. Zhang, J. Zhang, R. Wang, Z. Liu. *Carbon* **42**, 1455 (2004).
41. X. Zhang, Z. Lu, M. Wen, H. Liang, J. Zhang, Z. Liu. *J. Phys. Chem. B* **109**, 1101 (2005).
42. J. Deng, X. Ding, W. Zhang, Y. Peng, J. Wang, X. Long, P. Li, A. S. C. Chan. *Eur. Polym. J.* **38**, 2497 (2002).
43. S. J. Park, S. Y. Park, M. S. Cho, H. J. Choi, J. Joo. *Mol. Cryst. Liq. Cryst.* **425**, 299 (2004).
44. Y. Yu, B. Che, Z. Si, L. Li, W. Chen, G. Xue. *Synth. Met.* **150**, 271 (2005).
45. M Panhuis, R. Sainz, P. C. Innis, L. A. P. Kane-Maguire, A. M Benito, M. T. Artinez, S. E. Moulton, G. G. Wallace, W. K. Maser. *J. Phys. Chem. B* **109**, 22725 (2005).
46. R. Sainz, W. R. Samll, N. A. Young, C. Valles, A. M. Benito, W. K. Maser, M. Panhuis. *Macromolecules* **39**, 7324 (2006).
47. X. Zhang, W. Song, P. J. F. Harris, G. R. Mitchell, T. T. T. Bui, A. F. Drake. *Adv. Mater.* **19**, 1079 (2007).
48. H. Zang, H. X. Li, H. M. Cheng. *J. Phys. Chem. B* **110**, 9095 (2006).
49. M. G. Markoic, J. G. Matisons, R. Cervini, G. P. Simon, P. M. Fredericks. *Chem. Mater.* **18**, 6258 (2006).
50. H. Mi, X. Zhang, S. An, X. Ye, S. Yang. *Electrochem. Commun*. **9**, 2859 (2007).
51. K. P. Lee, A. I. Gopalan, P. Santhosh, S. H. Lee, Y. C. Nho. *Comp. Sci. Technol.* **67**, 811 (2007).
52. K. R. Reddy, K. P. Lee, A. I. Gopalan, M. S. Kim, A. M. Showkat, Y. C. Nho. *J. Polym. Sci., Part A* **44**, 3355 (2006).
53. M. Wu, G. A. Snook, V. Gupta, M. Shaffer, D. J. Fray, G. Z. Chen. *J. Mater. Chem*. **15**, 2297 (2005).
54. J. E. Huang, X. H. Li, J. C. Xu, H. L. Li. *Carbon* **41**, 2731 (2003).
55. S. E. Kooi, U. Schlecht, M. Burghard, K. Kern. *Angew. Chem., Int. Ed*. **41**, 1353 (2002).

56. K. Balasubramanian, M. Friedrich, C. Jiang, Y. Fan, A. Mews, M. Burghard, K. Kern. *Adv. Mater*. **15**, 1515 (2003).
57. F. Qu, M. Yang, J. Jiang, G. Shen, R. Yu. *Anal. Biochem.* **344**, 108 (2005).
58. P. Santhosh, K. M. Manesh, K. P. Lee, A. I. Gopalan. *Electroanalysis* **18**, 894 (2006).
59. X. Zhang, W. Song, P. J. F. Harris, G. R. Mitchell. *Chem. Phys. Chem*. **8**, 1766 (2007).
60. D. Wei, C. Kvarnström, T. Lindfors, A. Ivaska. *Electrochem. Commun.* **8**, 1563 (2006).
61. D. Wei, C. Kvarnstrom, T. Lindfors, A. Ivaska. *Electrochem. Commun*. **9**, 206 (2007).
62. V. Gupta, N. Miura. *J. Power Sources* **157**, 616 (2006).
63. V. Gupta, N. Miura. *Electrochim. Acta* **52**, 1721 (2006).
64. N. F. Anglada, M. Kaempgen, V. Skakalova, U. D. Weglikowska, S. Roth. *Diamond Relat. Mater.* **13**, 256 (2004).
65. N. F. Anglada, V. Gomis, Z. E. Hachemi, U. D. Weglikovska, M. Kaempgen, S. Roth. *Phys. Status Solidi (a)* **203**, 1082 (2006).
66. P. Gajendran, R. Saraswathi. *J. Phys. Chem. C* **111**, 11320 (2007).
67. Y. Lin, X. Cui. *J. Mater. Chem*. **16**, 582 (2006).
68. P. J. Kulesza, M. Skunik, B. Baranowska, K. Miecznikowski, M. Chojak, K. Karnicka, F. Frackowiak, F. Beguin, A. Kuhn, M. H. Delville, B. Starobrzynska, A. Ernst. *Electrochim. Acta* **51**, 2373 (2006).
69. P. S. M. Shaffer, X. Fan, A. H. Windle. *Carbon* **36**, 1603 (1998).
70. P. Gajendran, R. Saraswathi. Unpublished results.
71. G. Wu, L. Li, J. H. Li, B. Q. Xu. *J. Power Sources* **155**, 118 (2006).
72. D. J. Guo, H. L. Li. *J. Solid State Electrochem.* **9**, 445 (2005).
73. E. N. Konyushenko, J. Stejskal, M. Trchova, J. Hradil, J. Kovarova, J. Prokes, M. Cieslar, J. Y. Hwang, K. H. Chen, I. Sapurina. *Polymer* **47**, 5715 (2006).
74. A. Hassanien, M. Gao, M. Tokumoto, L. Dai. *Chem. Phys. Lett.* **342**, 479 (2001).
75. R. Sainz, A. M. Benito, M. T. Martinez, J. F. Galindo, J. Stores, A. M. Baro, B. Corraze, O. Chauvet, W. K. Maser. *Adv. Mater*. **17**, 278 (2005).
76. R. Sainz, A. M. Benito, M. T. Martinez, J. F. Galindo, J. Stores, A. M. Baro, B. Corraze, O. Chauvet, A. B. Dalton, R. H. Baughman, W. K. Maser. *Nanotechnology* **16**, S150 (2005).
77. Y. Ma, S. R. Ali, A. S. Dodoo, H. He. *J. Phys. Chem. B* **110**, 16359 (2006).
78. H. Zengin, W. Zhou, J. Jin, R. Czerw, D. W. Smith, J. L. Echegoyen, D. L. Carroll, S. H. Foulger, J. Ballato. *Adv. Mater.* **14**, 1480 (2002).
79. S. Lefrant, M. Baibarac, I. Baltog, J. Y. Mevellec, C. Godon, O. Chauvet. *Diamond Relat. Mater*. **14**, 867 (2005).
80. W. Feng, X. D. Ba, Y. Q. Lian, J. Liang, X. G. Wang, K. Yoshino. *Carbon* **41**, 1551 (2003).
81. Y. Long, Z. Chen. *Appl. Phys. Lett.* **85**, 1796 (2004).
82. H. Nakamatsu, E. Itoh, K. Miyairi. *Mol. Cryst. Liq. Cryst*. **472**, 485 (2007).
83. E. Bekyarova, M. E. Itkis, N. Cabrea, B. Zhao, A. Yu, J. Gao, R. C. Haddon. *J. Am. Chem. Soc*. **127**, 5990 (2005).
84. P. C. Ramamurthy, W. R. Harrell, R. V. Gregory, B. Sadanadan, A. M. Rao. *Polym. Eng. Sci.* **44**, 28 (2004).
85. P. C. Ramamurthy, A. M. Malshe, W. R. Harrel, R. V. Gregory, K. McGuire, A. M. Rao. *Solid-State Electron*. **48**, 2019 (2004).
86. C. Nastase, F. Nastase, A. Vaseashta, I. Stamatin. *Prog. Solid State Chem*. **34**, 181 (2006).
87. M. V. Kulkarni, A. K. Viswanath. *J. Macromol. Sci., Pure Appl. Chem*. **41**, 1173 (2004).
88. V. Mottaghitalab, G. M. Spinks, G. G. Wallace. *Synth. Met.* **152**, 77 (2005).
89. V. Mottaghitalab, B. Xi, G. M. Spinks, G. G. Wallace. *Synth. Met*. **156**, 796 (2006).
90. P. C. Ramamurthy, W. R. Harrell, R. V. Gregory, B. Sadanadan, A. M. Rao. *J. Electrochem. Soc*. **151**, G502 (2004).
91. S. J. Park, S. Y. Park, M. S. Cho, H. J. Choi, M. S. John. *Synth. Met*. **152**, 337 (2005).

92. H. J. Choi, S. J. Park, S. T. Kim, M. S. Jhon. *Diamond Relat. Mater*. **14**, 766 (2005).
93. C. S. Choi, S. J. Park, H. J. Choi. *Curr. Appl. Phys*. **7**, 352 (2007).
94. E. N. Konyushenko, N. E. Kazantseva, J. Stejskal, M. Trchova, J. Kovarova, I. Sapurina, M. M. Tomishko, O. V. Demicheva, J. Prokes. *J. Magn. Magn. Mater*. **320**, 231 (2008).
95. R. Saraswathi. *17th International Symposium on Fine Chemistry and Functional Polymers (FCFP-XVII) & IUPAC 3rd International Symposium on Novel Materials and Synthesis (NMS-III)*, 17–21 October 2007, Shanghai, China, J. Fudan University (Natural Science), **46**, 691 (2007).
96. C. Y. Wang, V. Mottaghitalab, C. O. Too, G. M. Spinks, G. G. Wallace. *J. Power Sources* **163**, 1105 (2007).
97. S. R. Sivakkumar, D. W. Kim. *J. Electrochem. Soc*. **154**, A134 (2007).
98. S. R. Sivakkumar, D. R. MacFarlane, M. Forsyth, D. W. Kim. *J. Electrochem. Soc.* **154**, A834 (2007).
99. P. Novák, K. Müller, K. S. V. Santhanam, O. Haas. *Chem. Rev.* **97**, 283 (1997).
100. B. E. Conway. *Electrochemical Supercapacitors: Scientific Fundamentals and Technological Applications*, pp. 299–334, Kluwer Academic/Plenum, New York (1999).
101. E. Frackowiak. In *Dekker Encyclopaedia of Nanoscience and Nanotechnology*, J. A. Schwarz, C. I. Contescu, K. Putyera (Eds.), C, 537–546, Taylor & Francis (2004).
102. M. Hughes. In *Dekker Encyclopaedia of Nanoscience and Nanotechnology*, J. A. Schwarz, C. I. Contescu, K. Putyera (Eds.), C, 447–459, Taylor & Francis (2004).
103. V. V. N. Obreja. *Physica E: Low-Dimen. Syst. Nanostruct.* **9**, 44 (2007).
104. A. K. Shukla, S. Sampath, K. Vijaymohanan. *Curr. Sci*. **79**, 1656 (2002).
105. K. R. Prasad, N. Munichandraiah. *J. Power Sources* **112**, 443 (2002).
106. E. Frackowiak, F. Beguin. *Carbon* **40**, 1775 (2002).
107. Y. K. Zhou, B. He, W. Zhou, J. Huang, X. Li, B. Wu, H. Li. *Electrochim. Acta* **49**, 257 (2004).
108. Y. K. Zhou, B. L. He, W. J. Zhou, H. L. Li. *J. Electrochem. Soc.* **151**, A1052 (2004).
109. J. Jang, J. Bae, M. Choi, S. H. Yoon. *Carbon* **43**, 2730 (2005).
110. V. Khomenko, E. Frackowiak, F. Beguin. *Electrochim. Acta* **50**, 2499 (2005).
111. M. Deng, B. Yang, Y. Hu. *J. Mater. Sci.* **40**, 5021 (2005).
112. S. R. Sivakkumar, W. J. Kim, J. A. Choi, D. R. MacFarlane, M. Forsyth, D. W. Kim. *J. Power Sources* **171**, 1062 (2007).
113. C. Peng, J. Jin, G. Z. Chen. *Electrochim. Acta* **53**, 525 (2007).
114. M. Wu, L. Zhang, D. Wang, J. Gao, S. Zhang. *Nanotechnology* **19**, 1 (2007).
115. K. M. Manesh, P. Santhosh, A. I. Gopalan. K. P. Lee. *Electroanalysis* **18**, 1564 (2006).
116. P. Santhosh, A. I. Gopalan, K. P. Lee. *J. Catal.* **238**, 177 (2006).
117. J. Shi, Z. Wang, H. L. Li. *J. Mater. Sci.* **42**, 539 (2007).
118. P. Gajendran, R. Saraswathi. *Proc. 2nd International Conf. on Emerging Adaptive Systems and Technologies*, p. 183, Kumaracoil, Tamilnadu, India, 25–27 October (2007).
119. J. Shi, D. J. Guo, Z. Wang, H. L. Li. *J. Solid State Electrochem.* **9**, 634 (2005).
120. Z. Z. Zhu, Z. Wang, H. L. Lin. *Appl. Surf. Sci*. **254**, 2934 (2008).
121. Z. Wang, Z. Z. Zhu, J. Shi, H. L. Li. *Appl. Surf. Sci*. **253**, 8811 (2007).
122. Y. Qiao, C. M. Li, S. J. Bao, Q. L. Bao. *J. Power Sources* **170**, 79 (2007).
123. H. Bai, G. Shi. *Sensors* **7**, 267 (2007).
124. D. D. Borole, U. R. Kaapadi, P. P. Mahulikar, D. G. Hundiwale. *J. Mater. Sci*. **9**, 1 (2006).
125. M. Gerard, A. Chaubey, B. D. Malhotra. *Biosens. Bioelectron.* **17**, 345 (2002).
126. B. D. Malhotra, A. Chaubey, S. P. Singh. *Anal. Chim. Acta* **578**, 59 (2006).
127. Q. Zhao, Z. Gan, Q. Zhuang. *Electroanalysis* **14**, 1609 (2002).
128. S. Sherigara, W. Kutner, F. D. Souza. *Electroanalysis* **15**, 753 (2003).
129. Y. Lin. S. Taylor, H. Li, A. S. Fernando, L. Qu, W. Wang, L. Gu, B. Zhou, Y. P. Sun. *J. Mater. Chem*. **14**, 527 (2004).

130. K. Gong, Y. Yan, M. Zhang, L. Su, S. Xiong, L. Mao. *Anal. Sci*. **21**, 1383 (2005).
131. J. J. Gooding. *Electrochim. Acta* **50**, 3049 (2005).
132. P. He, Y. Xu, Y. Fang. *Microchim. Acta* **152**, 175 (2006).
133. G. G. Wildgoose, C. E. Banks, H. C. Leventis, R. G. Compton. *Microchim. Acta* **152**, 187 (2006).
134. A. Merkoci. *Microchim. Acta* **152**, 157 (2006).
135. G. A. Rivas, M. D. Rubianes, M. C. Rodríguez, N. F. Ferreyra, G. L. Luque, M. L. Pedano, S. A. Miscoria, C. Parrado. *Talanta* **74**, 291 (2007).
136. S. N. Kim, J. F. Rusling, F. Papadimitrakopoulos. *Adv. Mater*. **19**, 3214 (2007).
137. M. Kaempgen, S. Roth. *J. Electroanal. Chem.* **586**, 72 (2006).
138. N. F. Anglada, M. Kaempgen, S. Roth. *Phys. Status Solidi B* **243**, 3519 (2006).
139. L. Valentini, V. Bavastrello, E. Stura, I. Armentano, C. Nicolini, J. M. Kenny. *Chem. Phys. Lett.* **383**, 617 (2004).
140. L. Valentini, J. M. Kenny. *Polymer* **46**, 6715 (2005).
141. Y. Li, H. Wang, X. Cao, M. Yuan, M. Yang. *Nanotechnology* **19**, 1 (2008).
142. Y. Wanna, N. Srisukhumbowornchai, A. Tuantranont, A. Wisitsoraat, N. Thavarungkul, P. Singjai. *J. Nanosci. Nanotechnol*. **6**, 3893 (2006).
143. P. Santhosh, K. M. Manesh, A. I. Gopalan, K. P. Lee. *Sens. Actuators, B* **125**, 92 (2007).
144. M. Guo, J. Chen, J. Li, B. Tao, S. Yao. *Anal. Chim. Acta* **532**, 71 (2005).
145. Y. Lin, X. Cui. *Chem. Commun*. 2226 (2005).
146 X. Gao, W. Wei, L. Yang, M. Guo. *Electroanalysis* **18**, 485 (2006).
147. M. Li, L. Jing. *Electrochim. Acta* **52**, 3250 (2007).
148. E. Granot, B. Basnar, Z. Cheglakov, E. Katz, I. Willner. *Electroanalysis* **18**, 26 (2006).
149. J. Liu, S. Tian, W. Knoll. *Langmuir* **21**, 5596 (2005).
150. J. Zeng, X. Gao, W. Wei, X. Zhai, J. Yin, L. Wu, X. Liu, K. Liu, S. Gong. *Sens. Actuators, B* **120**, 595 (2007).
151. S. R. Ali, Y. Ma, R. R. Parajuli, Y. Balogun, W. Y. C. Lai, H. He. *Anal. Chem.* **79**, 2583 (2007).
152. S. R. Ali, R. R. Parajuli, Y. Ma, Y. Balogun, H. He. *J. Phys. Chem. B* **111**, 12275 (2007).
153. T. Yin, W. Wei, J. Zeng. *Anal. Bioanal. Chem*. **386**, 2087 (2006).
154. Z. Wang, J. Yean, M. Li, D. Han, Y. Zhang, Y. Shen, L. Niu, A. Tvaska. *J. Electroanal. Chem.* **599**, 121 (2007).
155. D. Pan, J. Chen, S. Yao, W. Tao, L. Nie. *Anal. Sci.* **21**, 367 (2005).
156. P. Santhosh, K. M. Manesh, A. I. Gopalan, K. P. Lee. *Anal. Chim. Acta* **575**, 32 (2006).
157. Y. Zou, L. Sun, F. Xu. *Talanta* **72**, 437 (2007).
158. Y. Zou, L. Sun, F. Xu. *Biosens. Bioelectron.* **22**, 2669 (2007).
159. K. Kaneto, M. Kaneko, Y. Min. A. G. MacDiarmid. *Synth. Met.* **71**, 2211 (1995).
160. E. Smela, W. Lu, B. R. Mattes. *Synth. Met*. **151**, 25 (2005).
161. G. M. Spinks, L. Liu, G. G. Wallace, D. Zhou. *Adv. Funct. Mater*. **12**, 437 (2002).
162. S. Hara, T. Zama, W. Takashima, K. Kaneto. *Polym. J*. **36**, 151 (2004).
163. R. H. Baughman, C. Cui, A. A. Zakhidov, Z. Iqbal, J. N. Barisci, G. M. Spinks. G. G. Wallace, A. Mazzoldi, D. D. Rossa, A. G. Rinzler, O. Jaschinski, S. Roth, M. Kertesz. *Science* **284**, 1340 (1999).
164. Y. Yun, V. Shanov, Y. Tu, M. Schulz, S. Yarmolenko, S. Neralla, J. Sankar S. Subramaniam. *Nano Lett.* **6**, 689 (2006).
165. B. J. Landi, R. P. Raffaelle, M. J. Heben, J. L. Alleman, W. VanDerveer, T. Gennett. *Nano Lett.* **2**, 1329 (2002).
166. X. Yu, R. Rajamani, K. A. Stelson, T. Cui. *Sen. Actuators, A* **132**, 626 (2006).
167. M. Tahhan, V. T. Truong, G. M. Spinks, G. G. Wallace. *Smart Mater. Struct*. **12**, 626 (2003).
168. G. M. Spinks, B. Xi, V. T. Truong, G. G. Wallace. *Synth. Met*. **151**, 85 (2005).
169. G. M. Spinks, V. Mottaghitalab, M. B. Samani, P. G. Whitten, G. G. Wallace. *Adv. Mater*. **18**, 637 (2006).

170. G. M. Spinks, S. R. Shin, G. G. Wallace, P. G. Whitten, I. Y. Kim, S. I. Kim, S. J. Kim. *Sens. Actuators, B* **21**, 616 (2007).
171. S. Yun, J. Kim, Z. Ounaies. *Smart Mater. Struct*. **15**, N61 (2006).
172. S. Yun, J. Kim. *Synth. Met*. **157**, 523 (2007).
173. S. Yun, J. Kim. *J. Phys. D: Appl. Phys*. **39**, 2580 (2006).
174. C. Klinke, J. Chen, A. Afzali, P. Avouris. *Nano Lett*. **5**, 555 (2005).
175. P. C. Ramamurthy, W. R. Harell, R. V. Gregory, B. Sadanadan, A. M. Rao. *Synth. Met.* **137**, 1497 (2003).
176. G. B. Blanchet, C. R. Fincher, F. Gao. *Appl. Phys. Lett.* **82**, 1290 (2003).
177. M. Lefenfeld, G. Blanchet, J. A. Rogers. *Adv. Mater*. **15**, 1188 (2003).
178. W. R. Small, F. Masdarolomoor, G. G. Wallace, M. Panhuis. *J. Mater. Chem*. **17**, 4359 (2007).
179. M. Panhuis, J. Wu, S. A. Ashraf, G. G. Wallace. *Synth. Met*. **157**, 358 (2007).
180. L. Hu, G. Gruner, D. Li, R. B. Kaner, J. Cech. *J. Appl. Phys*. **101**, 1 (2007).